ALCATEL MATÁV Broadband Networks Inc. IEEE COMSOC

CWAS '97

International Workshop on Copper Wire Access Systems "Bridging the Last Copper Drop"

October 27–29, 1997, Budapest

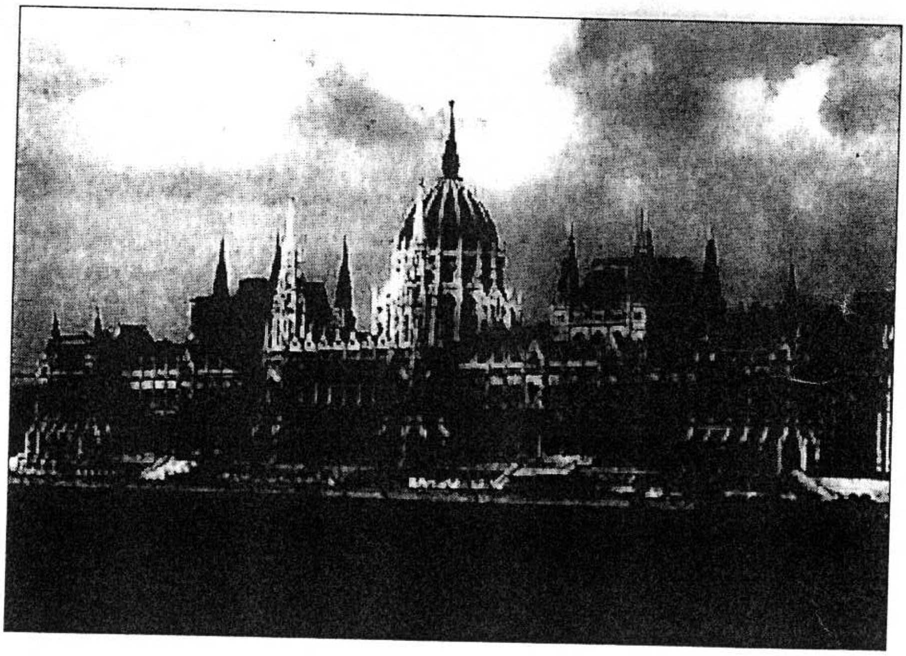

PROCEEDINGS

Panem

Performance Degradation of Multi-Carrier Systems Caused by an Insufficient Guard Interval Duration

Thierry Pollet[†], *Heidi Steendam* and *Marc Moeneclaey*

[†] Alcatel Telecom
Francis Wellesplein 1
B-2018 Antwerpen, Belgium
tel:+32 3 240 88 34, fax:+32 3 240 99 32

Communication Engineering Lab.
DIGCOM Research Group, University of Ghent
St-Pietersnieuwstraat 41, B-9000 Ghent, Belgium
tel: +32 9 264 34 12, fax: +32 9 264 42 95

***Abstract*—In multi-carrier transmission over a slowly time-varying dispersive channel, inter-symbol interference (ISI) is avoided by appending a guard time to each symbol. ISI free transmission is guaranteed provided that the guard time duration is longer than the channel impulse response. In addition, the orthogonality of the modulated carriers is maintained when the guard time consists of a periodic extension of the signal transmitted for each symbol. This paper analyses the structure of the ISI and the inter-carrier (ICI) interference which is present at the input of the decision device when the length of the composite impulse response exceeds the guard time duration. For multi-carrier transmission by means of modulated IDFT basis vectors, a simple expression for the ISI and ICI is derived. The study clarifies to which extent different carriers in the multi-carrier signal interfere. Based on the analysis, a symbol frame synchronization structure is proposed. The results are illustrated for high rate data transmission over copper wires where the capacity loss caused by the presence of ISI and ICI is computed.**

I. Introduction

In multi-carrier transmission, the (binary) information sequence is split in consecutive data frames. The bits belonging to each frame are assigned to the available subchannels (carriers) and mapped into symbols that modulate the carriers (Fig. 1). Discrete multitone (DMT) signaling performs modulation digitally by means of a set of orthogonal vectors $\{\overline{B}_k = (b_0^k \ldots, b_{2N-1}^k), k \in [0, .., 2N-1]\}$.

Denote a_m^k the (complex) symbol that modulates the k-th vector during the m-th frame. The transmitter generates the samples $s_m(n) = \sum_{k=0}^{2N-1} a_m^k b_n^k, n \in [0, .., 2N-1]$. In order to avoid interference between DMT frames during transmission over a dispersive channel, a prefix is appended to $s_m(n)$, $(\forall m)$, which consists of a repetition of the last ν samples. Finally, conversion from discrete-time to continuous-time domain is performed by feeding the generated sample sequence to a transmit filter $p(t)$ at the rate

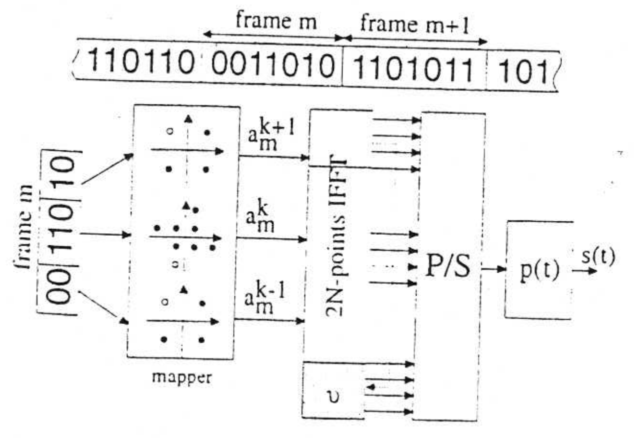

Fig. 1. Multi-carrier transmitter

$f_s = \frac{1}{T}$. Selecting the IDFT basis vectors ($b_n^k = e^{j2\pi\frac{kn}{2N}}$), the DMT signal can be generated by means of an inverse Fast Fourier Transform (IFFT) [1]. Hence, the DMT signal $s(t)$ can be expressed as

$$s(t) = \frac{1}{2N}\sum_{m=-\infty}^{+\infty}\sum_{k=0}^{2N-1} a_m^k \sum_{n=-\nu}^{2N-1} e^{j2\pi\frac{kn}{2N}} p(t-nT-m(2N+\nu)T) \quad (1)$$

Imposing $a_m^k = (a_m^{2N-k})^*, \forall k \in [1, .., N-1]$ [1], (1) yields a real baseband signal with DMT symbol period $(2N+\nu)T$ where the symbol a_m^k modulates the carrier at frequency $\frac{k}{2NT}$. In the sequel, it is assumed that the variance of the symbols is normalized to E_s (i.e. $E[\|a_m^k\|^2] = E_s$) if vector $\overline{B}_k$ is modulated and that $a_m^k = 0$ in case the k-th subchannel is not used.

At the receiver, the detection of the symbols $a_{m'}^{k'}, k' \in [0..N]$ is done as follows: the receiver filter output is sampled at the time instants $t = m'(2N+\nu)T + n'T + \Delta T$ with $n' \in [-\nu, 2N-1]$. The prefix samples are discarded and an FFT is performed on the remaining $2N$ real values. The offset between the receiver and transmitter symbol frame clock, ΔT, is provided by the symbol frame synchronization algorithm in order to make reliable decisions about the received symbols $a_{m'}^{k'}, k' \in [0, \ldots, N]$.

The signal at time instant $t = m'(2N+\nu)T + n'T + \Delta T$ can be expressed as

$$r_{n'+m'(2N+\nu)+\Delta} = \frac{1}{2N}\sum_{m=-\infty}^{+\infty}\sum_{k=0}^{2N-1}\sum_{n=-\nu}^{2N-1} a_m^k e^{j2\pi\frac{kn}{2N}} \cdot g((n'-n)T + (m'-m)(2N+\nu)T + \Delta T) + N_{m'}^{n'} \quad (2)$$

where $g(t)$ denotes the composite channel impulse response which consists of the cascade of the channel, the transmit filter and the receiver filter. The second term in (2) is the contribution of the (coloured) noise added to the DMT signal during transmission over the channel. The corresponding FFT outputs can be expressed as

$$\begin{aligned}\mathrm{FFT}_{m'}^{k'} &= \sum_{n'=0}^{2N-1} r_{n'+m'(2N+\nu)+\Delta} e^{-j\frac{2\pi}{2N}k'n'} \\ &= \sum_{m=-\infty}^{+\infty}\sum_{k=0}^{2N-1} a_m^k z_{m'}^{k'}(m,k) + \tilde{N}_{m'}^{k'}\end{aligned}$$

with

$$z_{m'}^{k'}(m,k) =$$

[1] For the carrier at d.c. and $\frac{1}{2T}$ (k=0, k=N) the transmitted symbols are real ($a_m^k = (a_m^k)^*$).

$$\frac{1}{2N}\sum_{n''=-(2N-1)}^{2N-1+\nu} g(n''T+(m'-m)T+\Delta T)e^{-j\frac{2\pi}{2N}kn''}.$$

$$\sum_{n=L(n'')}^{U(n'')} e^{j\frac{2\pi}{2N}(k-k')n},$$

$n'' = n' - n$, and

$$L(n'') = \begin{cases} -n'' & -(2N-1) \le n'' \le \nu \\ -\nu & \nu < n'' \le 2N-1+\nu \end{cases}$$

$$U(n'') = \begin{cases} 2N-1 & -(2N-1) \le n'' < 0 \\ 2N-1-n'' & 0 \le n'' \le 2N-1+\nu \end{cases}$$

The signals presented to the decision device are corrupted by inter-frame and intra-frame interference. In the assumption that the composite impulse response is restricted to $-(2N-1-\Delta)T \le t \le (2N-1+\nu+\Delta)T$, the FFT output contains contributions only from the transmitted symbols $\{a^{k'}_{m'-1}, a^{k'}_{m'}, a^{k'}_{m'+1}\}, k' \in [0,..,2N-1]$. In the sequel it is shown how the ICI and ISI contribution to the decision variables $\mathrm{FFT}^{k'}_{m'}$ easily can be expressed as function of $2N$ point FFT transforms on segments of the sampled composite channel impulse response $g(t)$. The analysis gives an understanding to which extent the subchannels interfere. The remainder of the paper is organized as follows. In section II, the signal at the FFT output is decomposed into a useful component, inter-symbol interference and inter-carrier interference, respectively. In section III, a frame synchronization structure is derived which is based on minimizing the total ISI plus ICI power in the received signal. In section IV, the capacity reduction caused by the presence of ISI and ICI is illustrated for high rate DMT transmission over the copper wire. Finally, in section V, conclusions are drawn.

II. Decomposition of the Received Signal

A. The Useful Signal component

The useful signal component in $\mathrm{FFT}^{k'}_{m'}$ is the term proportional to $a^{k'}_{m'}$ and can be expressed as

$$a^{k'}_{m'}z^{k'}_{m'}(m',k') = a^{k'}_{m'}\sum_{n=-(2N-1)}^{2N-1+\nu} w(n)g((n+\Delta)T)e^{-j\frac{2\pi}{2N}k'n} \quad (3)$$

where $w(n)$ is depicted in Fig. 2. In case the impulse response duration is shorter than the guard time (i.e. $g(t) = 0$ for $t \ge (\nu+\Delta)T$ and $t \le \Delta T$) (3) can be written [2] as

$$\begin{aligned} a^{k'}_{m'}z^{k'}_{m'}(m',k') &= a^{k'}_{m'}\, G(z)z^{\Delta}\big|_{z=e^{j\frac{2\pi}{2N}k'}} \\ &= a^{k'}_{m'}\, G(z)z^{\Delta}\big|_{z=e^{j2\pi f_{k'}T}} \end{aligned} \quad (4)$$

where $f_{k'} = \frac{k'}{2NT}$ and $G(z)$ is the Z-transform of the sampled composite impulse response $g(t)$. Note that

$$G(e^{j2\pi fT}) = \frac{1}{T}\sum_{l=-\infty}^{+\infty} G(f+\frac{l}{T}).$$

and

$$G(e^{j2\pi fT})e^{j2\pi fT\Delta} = \frac{1}{T}\sum_{l=-\infty}^{+\infty} G(f+\frac{l}{T})e^{j2\pi(f+\frac{l}{T})T\Delta}.$$

$$f \in \left[-\frac{1}{2T}, \frac{1}{2T}\right]$$

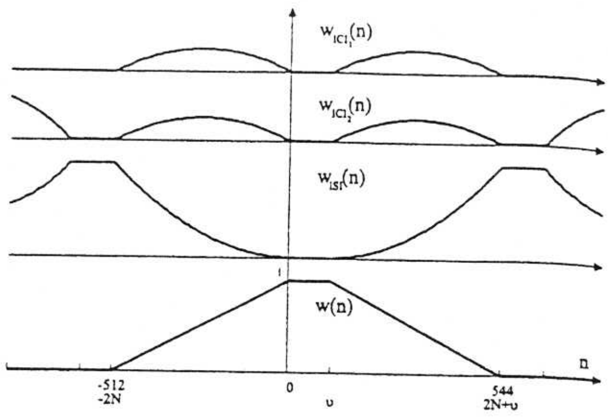

Fig. 2. The weight functions $w(n)$, $w_{ISI}(n)$, $w_{ICI_1}(n)$, $w_{ICI_2}(n)$

where $G(f)$ is the Fourier transform of $g(t)$. Hence (4) can be rewritten as

$$a^{k'}_{m'}z^{k'}_{m'}(m',k') = a^{k'}_{m'}\frac{1}{T}G(\frac{k'}{2NT})e^{j\frac{2\pi}{2N}k'\Delta}$$

provided that $G(f)$ is strictly band limited to $\left[-\frac{1}{2T}, \frac{1}{2T}\right]$.

When the composite channel impulse response is not restricted to the guard time, the useful signal can be expressed as

$$\begin{aligned} &a^{k'}_{m'}z^{k'}_{m'}(m',k') = \\ &a^{k'}_{m'}\Big[z^{\Delta}\Big(G(z)+\frac{1}{2N}(z\dot{G}_1(z)+(\Delta+\nu)\dot{G}_1(z) \\ &-z\dot{G}_2(z)-\Delta G_2(z))\Big)\Big]\Big|_{z=e^{j2\pi f_{k'}T}} \end{aligned} \quad (5)$$

where $G_1(z)$ en $G_2(z)$ are the Z-transforms of sampled versions of $g_1(t)$ en $g_2(t)$ defined as:

$$g_1(t) = \begin{cases} g(t) & (\nu+\Delta)T < t \le (2N-1+\Delta+\nu)T \\ 0 & \text{elsewhere} \end{cases}$$

$$g_2(t) = \begin{cases} g(t) & -((2N-1)-\Delta)T \le t < \Delta T \\ 0 & \text{elsewhere} \end{cases}$$

$g_1(t)$ and $g_2(t)$ are refered to as the tail and the head of the composite impulse response $g(t)$ hereafter.

B. Calculation of the ISI

In case the composite impulse response is longer than the guard time, ICI and ISI will be added to the FFT outputs. $\mathrm{ISI}(m',k')$ is the inter-frame interference originating from the symbols modulating carrier $\frac{k'}{2NT}$. The inteference consists of the contribution from the symbols $a^{k'}_{m'+1}$ and $a^{k'}_{m'-1}$ to the decision variable $\mathrm{FFT}^{k'}_{m'}$ which is used to estimate the transmitted symbol $a^{k'}_{m'}$. $\mathrm{ISI}(m',k')$ can be written as

$$\begin{aligned} &\mathrm{ISI}(m',k') \\ &= a^{k'}_{m'-1}z^{k'}_{m'}(m'-1,k') + a^{k'}_{m'+1}z^{k'}_{m'}(m'+1,k') \\ &= a^{k'}_{m'-1}\frac{1}{2N}\left[\sum_{n=\nu+1}^{2N+\nu}(n-\nu)g((n+\Delta)T)e^{-j\frac{2\pi}{2N}k'(n-\nu)}\right] \\ &- a^{k'}_{m'+1}\frac{1}{2N}\left[e^{-j\frac{2\pi}{2N}k'\nu}\sum_{n=-2N}^{-1} ng((n+\Delta)T)e^{-j\frac{2\pi}{2N}k'n}\right] \end{aligned} \quad (6)$$

$$= a^{k'}_{m'-1} e^{-j\frac{2\pi}{2N}k'} \frac{1}{2N}\left[\mathrm{FFT}_1(k') + \mathrm{FFT}_3(k')\right]$$
$$+ a^{k'}_{m'+1} e^{-j\frac{2\pi}{2N}k'\nu} \frac{1}{2N}\left[2N\mathrm{FFT}_2(k') - \mathrm{FFT}_4(k')\right]$$
$$\approx \frac{a^{k'}_{m'-1}}{2NT}\left[-(\nu+\Delta)G_1(\frac{k'}{2NT}) + \frac{j}{2\pi T}\dot{G}_1(\frac{k'}{2NT})\right] e^{j\frac{2\pi}{2N}k'(\nu+\Delta)}$$
$$+ \frac{a^{k'}_{m'+1}}{2NT}\left[\Delta G_2(\frac{k'}{2NT}) - \frac{j}{2\pi T}\dot{G}_2(\frac{k'}{2NT})\right] e^{-j\frac{2\pi}{2N}k'(\nu-\Delta)}$$

where

$$\mathrm{FFT}_1(k) = \sum_{n=0}^{2N-1} g((n+\nu+1+\Delta)T)e^{-j\frac{2\pi}{2N}kn}$$
$$\mathrm{FFT}_2(k) = \sum_{n=0}^{2N-1} g((n-2N+\Delta)T)e^{-j\frac{2\pi}{2N}kn}$$
$$\mathrm{FFT}_3(k) = \sum_{n=0}^{2N-1} ng((n+\nu+1+\Delta)T)e^{-j\frac{2\pi}{2N}kn}$$
$$\mathrm{FFT}_4(k) = \sum_{n=0}^{2N-1} ng((n-2N+\Delta)T)e^{-j\frac{2\pi}{2N}kn}$$

Observe that $\mathrm{FFT}_1(k)$ and $\mathrm{FFT}_2(k)$ ($k \in [0,..,2N-1]$), are the FFT of the (sampled) tail and head.

C. Calculation of the ICI

Two types of inter-carrier interference can be distinguished: intra-frame ICI (ICI_1) and inter-frame ICI (ICI_2). $\mathrm{ICI}_1(m',k',k)$ denotes the interference from the symbol $a^k_{m'}, k \neq k'$, the symbols modulating the k-th basis vector at the m'-th symbol period:

$$\mathrm{ICI}_1(m',k',k) = a^k_{m'} z^k_{m'}(m',k') = a^k_{m'} \sum_{n=-(2N-1)}^{2N+\nu-1} v(n)$$

where

$$2Nv(n) = \begin{cases} -(2N-1) \le n \le -1 & g((n+\Delta)T)e^{-j\frac{2\pi}{2N}kn}W(n) \\ 0 \le n \le \nu & 0 \\ \nu+1 \le n \le 2N+\nu-1 & g((n+\Delta)T)e^{-j\frac{2\pi}{2N}((k-k')\nu+W(n))} \end{cases}$$

with

$$W(n) = \frac{1-e^{-j2\pi(k-k')w(n)}}{1-e^{-j\frac{2\pi}{2N}(k-k')}};$$

Defining (Fig. 3)

$$A(k-k') = \left[1-e^{-j\frac{2\pi}{2N}(k-k')}\right]^{-1},$$

$\mathrm{ICI}_1(m',k',k)$, becomes

$$\mathrm{ICI}_1(m',k',k) = A(k-k')\frac{a^k_{m'}}{2N}\cdot$$
$$\left[e^{-j\frac{2\pi}{2N}k\nu}\left[e^{-j\frac{2\pi}{2N}k'}\mathrm{FFT}_1(k') - e^{-j\frac{2\pi}{2N}k}\mathrm{FFT}_1(k)\right]\right.$$
$$\left. + \left[\mathrm{FFT}_2(k) - \mathrm{FFT}_2(k')\right]\right]$$
$$\approx A(k-k')\frac{a^k_{m'}}{2NT}\cdot$$
$$\left[-G_1(\frac{k}{2NT})e^{j\frac{2\pi}{2N}k\Delta} + G_1(\frac{k'}{2NT})e^{-j\frac{2\pi}{2N}(k\nu-k'(\nu+\Delta))}\right.$$
$$\left. + G_2(\frac{k}{2NT})e^{j\frac{2\pi}{2N}k\Delta} - G_2(\frac{k'}{2NT})e^{j\frac{2\pi}{2N}k'\Delta}\right] \quad (7)$$

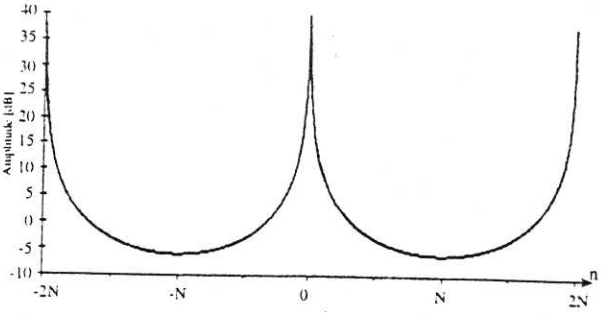

Fig. 3. $|A(n)|$ as function of n

$\mathrm{ICI}_2(m',k',k)$ is the interference caused by the symbols a^k_{m-1} and a^k_{m+1} and can be written as

$$\mathrm{ICI}_2(m',k',k) = A(k-k')\frac{1}{2N}\cdot \quad (8)$$
$$\left[a^k_{m'-1}\left[e^{-j\frac{2\pi}{2N}k}\mathrm{FFT}_1(k) - e^{-j\frac{2\pi}{2N}k'}\mathrm{FFT}_1(k')\right]\right.$$
$$\left. + a^k_{m'+1}e^{-j\frac{2\pi}{2N}k\nu}\left[\mathrm{FFT}_2(k') - \mathrm{FFT}_2(k)\right]\right]$$
$$\approx -\frac{1}{2NT}A(k-k')(a^k_{m'-1}e^{j\frac{2\pi}{2N}k\nu}$$
$$\left[-G_1(\frac{k}{2NT})e^{j\frac{2\pi}{2N}k\Delta} + G_1(\frac{k'}{2NT})e^{-j\frac{2\pi}{2N}(k\nu-k'(\nu+\Delta))}\right]$$
$$+ a^k_{m'+1}e^{-j\frac{2\pi}{2N}k\nu}\left[G_2(\frac{k}{2NT})e^{j\frac{2\pi}{2N}k\Delta} - G_2(\frac{k'}{2NT})e^{j\frac{2\pi}{2N}k'\Delta}\right])$$

D. Discussion

Equation (6) implies that the ISI can be expressed in terms of the Fourier transform on the tail $g_1(t)$, head $g_2(t)$ and their derivates evaluated at the considered carrier frequency $\frac{k'}{2NT}$. ICI (7,8) depends upon the Fourier transform of the head and the tail, taken at the useful carrier frequency $\frac{k'}{2NT}$ and the interfering frequency $\frac{k}{2NT}$. The weight function $|A(k-k')|$ in the equations bears out the intuition that interferers further away from the useful carrier interfere far less than nearby interferers. However, as will be illustrated in section IV, the effect of the channel transfer function may not be neglected. Comparing (7) with (8) reveals that except for the cross-product term

$$\frac{2}{(2NT)^2}E_s|A(k-k')|^2\Re\left(\left[-G_1(\frac{k}{2NT})e^{j\frac{2\pi}{2N}k\Delta}\right.\right.$$
$$\left. + G_1(\frac{k'}{2NT})e^{-j\frac{2\pi}{2N}(k\nu-k'(\nu+\Delta))}\right]$$
$$\left.\left[G_2(\frac{k}{2NT})e^{j\frac{2\pi}{2N}k\Delta} - G_2(\frac{k'}{2NT})e^{j\frac{2\pi}{2N}k'\Delta}\right]^*\right) \quad (9)$$

the inter-frame interference power from modulated carrier $\frac{k}{2NT}$ on $\frac{k'}{2NT}$ is equal to the intra-frame interference power attributed to that carrier. In many cases, the contribution of the cross-product to the $\mathrm{ICI}_1(m',k',k)$ power is small. Observe that the interference power from type ICI_2 is reciproke (i.e the interference power from carrier k on k' equals the interference power from carrier k' on k). From equations (7,8) is clear that the carrier k does not interfere when

$$a^k_{m-1}e^{j\frac{2\pi}{2N}k\nu} = a^k_m = a^k_{m+1}e^{-j\frac{2\pi}{2N}k\nu}. \quad (10)$$

Indeed, selecting the transmitted symbols as in (10) corresponds to the transmission of a sinusoid.

The *total* ISI, ICI_1 and ICI_2 power is defined as

$$V_{ISI}(\Delta) = \sum_{k'\in\Omega(i)} E[|ISI(m',k')|^2],$$

$$V_{ICI_1}(\Delta) = \sum_{k'\in\Omega(i)} \sum_{\substack{k\in\Omega(i)\\k\neq k'}} E[|ICI_1(m',k',k)|^2] \quad \text{and}$$

$$V_{ICI_2}(\Delta) = \sum_{k'\in\Omega(i)} \sum_{\substack{k\in\Omega(i)\\k\neq k'}} E[|ICI_2(m',k',k)|^2],$$

respectively where $\Omega(i)$ is the set of indices i of the modulated carriers $\frac{i}{2NT}$. When there are a small number of unmodulated carriers a close upperbound for $V_{ISI}(\Delta)$, $V_{ICI_1}(\Delta)$ and $V_{ICI_2}(\Delta)$ can be obtained by assuming *all* the carriers in the multi-carrier signal are modulated. It is shown in the appendix that $V_{ISI}(\Delta)$ can be written as

$$V_{ISI}(\Delta) = E_s \sum_{k'=0}^{2N-1} (|z_{m'}^{k'}(m'-1,k')|^2 + |z_{m'}^{k'}(m'-1,k')|^2)$$

$$= 2NE_s \sum_{n=-\infty}^{+\infty} w_{ISI}(n) g^2((n+\Delta)T)$$

Similarly, The total ICI_1, ICI_2 and total useful signal power, $V_U(\Delta)$, can be expressed as

$$V_{ICI_1}(\Delta) = 2NE_s \sum_{n=-\infty}^{+\infty} w_{ICI_1}(n) g^2((n+\Delta)T)$$

$$V_{ICI_2}(\Delta) = 2NE_s \sum_{n=-\infty}^{+\infty} w_{ICI_2}(n) g^2((n+\Delta)T)$$

$$V_U(\Delta) = E_s \sum_{k'=0}^{2N-1} |z_{m'}^{k'}(m',k')|^2$$

$$= 2NE_s \sum_{n=-\infty}^{+\infty} w^2(n) g^2((n+\Delta)T)$$

where the weight functions are depicted in Fig. 2. It is concluded that on the average, the ISI power is much smaller than the ICI power and that $V_{ICI_1}(\Delta) \approx V_{ICI_2}(\Delta)$.

III. Symbol Frame Synchronization

In order to recover the transmitted DMT symbols, the receiver processes blocks of $2N+\nu$ contiguous samples. The symbol frame synchronizer estimates symbol boundaries. In [4] the authors propose a Maximum Likelihood based algorithm, which exploits the presence of the cyclic prefix. Alternatively, the synchronizer may attempt to maximize the capacity what is equivalent to maximizing the *geometric* SNR [7]. A simple and robust synchronization structure can be obtained, based on minimizing the total ISI plus ICI power $V_{ISI}(\Delta) + V_{ICI_1}(\Delta) + V_{ICI_2}(\Delta)$. The weight functions satisfy the property $w^2(n) + w_{ICI_1}(n) + w_{ICI_2}(n) + w_{ISI}(n) = 1, \forall n$. Hence minimizing the ISI and ICI power with respect to Δ is equivalent to maximizing the total useful signal power. The proposed frame synchronization algorithm can be summarized as follows. Estimate the composite channel impulse response $g(t)$. This can be achieved during an initialization phase where unmodulated carriers are transmitted and no guard band is inserted. In a practical receiver implementation, $g(t)$ is measured only at the time instants $g(nT)$. Find k for which $\sum_{n=-\infty}^{+\infty} w^2(n-k) g^2(nT)$ is maximized. Then kT yields the optimal choice of ΔT within a sample period $]-T, T[$. This approach is suited for coarse grain acquisition. The synchronization algorithm can be simplified by replacing $w^2(n)$ by a brick-wall window of length $\nu + 1$ (samples). Hence, the synchronizer seeks the part of the channel impulse response of duration νT that contains the largest energy. Fine grain synchronization (during tracking mode) can be performed as described in [6].

IV. Capacity Reduction caused by ISI and ICI

In case the channel varies slowly with respect to the symbol duration, the achievable transmission rate for a given bit error rate (BER) can be optimized by selecting a constellation size for each modulated carrier depending upon the SNR at the receiver on this carrier. The measured SNR values are communicated to the transmitter which allocates the number of bits $b_{k'}$ on the carrier $\frac{k'}{2NT}$ according to the rule [8]

$$b_{k'} = \lfloor \log_2(1 + \frac{SNR(\frac{k'}{2NT})G}{\Gamma M}) \rfloor \quad (11)$$

where Γ depends on the required BER ($\Gamma = 9.55$ for BER $= 10^{-7}$), M denotes the system SNR margin and G the coding gain. The SNR at carrier $\frac{k'}{2NT}$ can be written as

$$SNR(\frac{k'}{2NT}) = \frac{E_s E[|z_{m'}^{k'}(m',k')|^2]}{E[|\tilde{N}_{m'}^{k'}|^2] + E[|ISI(m',k')|^2] + \sum_{k\neq k'} E[|ICI_{\frac{1}{2}}(m',k',k)|^2]}$$

The resulting capacity becomes $\frac{2N}{2N+\nu}\frac{1}{2NT}\sum_{k'=0}^{N} b_{k'}$. The first factor indicates the capacity loss due to the insertion of the prefix. The capacity is to be compared with the maximal achievable data rate which is obtained when the receiver is able to cancel all the ICI and ISI without increasing the noise variance $E[|\tilde{N}_{m'}^{k'}|^2]$.

A. Application to VDSL transmission

In a fibre-to-the-curb access network, the subscriber is connected by means of a copper wire to the optical network unit (ONU) which in turn is connected to the central office by fibre. Because of the short wire length bit rates of tens of Mb/sec are achievable (Very High Rate Digital Subscriber Loop transmission). As the ONU services several subscribers, the copper wires are grouped in a binder. This yields electromagnetic interference when the lines carry signals. In the simultations, we assume Far End Crosstalk (FEXT) attributed to 12 wires in the binder. The FEXT power spectral desity is modeled as $K_{FEXT} f^2 d S(f) |G(f)|^2$ where $K_{FEXT} = 3E^{-16}(\frac{12}{49})^{0.6} Hz^{-2} Km^{-1}$, $S(f)$ is the transmit psd of the interferer, d the length of the wire (in Km), and $G(f)$ is the composite channel transfer function. In addition, a background AWG noise with a one-sided psd of -140 dBm/Hz is taken into account. The DMT transceiver modulates 256 carriers ($2N = 512$) with a guard time length $\nu = 32$. The 10 lowest subchannels are not used for reasons of spectral compatibility with other services (e.g. BRA-ISDN, POTS). At the receiver and transmitter, a 5-th order Chebychev high pass filter (0.25 dB ripple, $f_{cut\text{-}off} = 375$KHz) splits the DMT signals from the coexisting services. The DMT signal occupies a transmission band up to 10 MHz ($f_s = 20$ MHz) with a power density mask of -60 dBm/Hz.

[1] $\lfloor x \rfloor$ denotes the largest integer smaller or equal to x

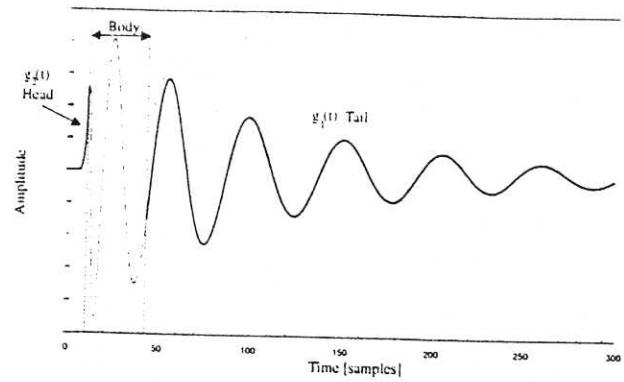

Fig. 4. The composite channel impulse response $g(t)$

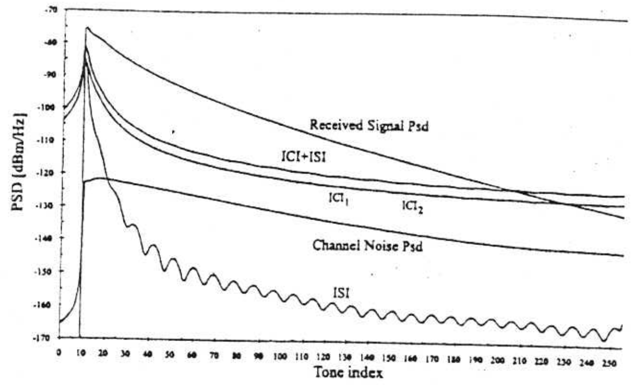

Fig. 6. Spectra of the received signals

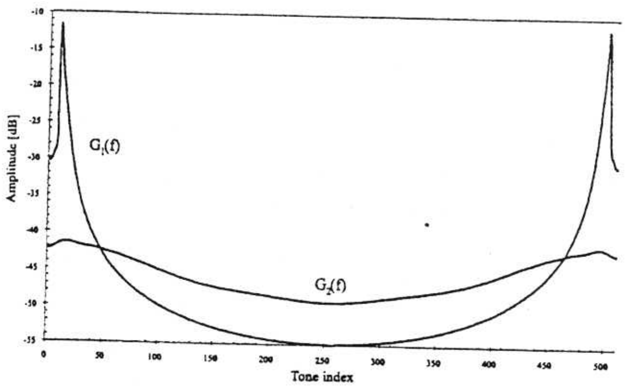

Fig. 5. Fourier Transform of head and tail $G_1(f)$, $G_2(f)$

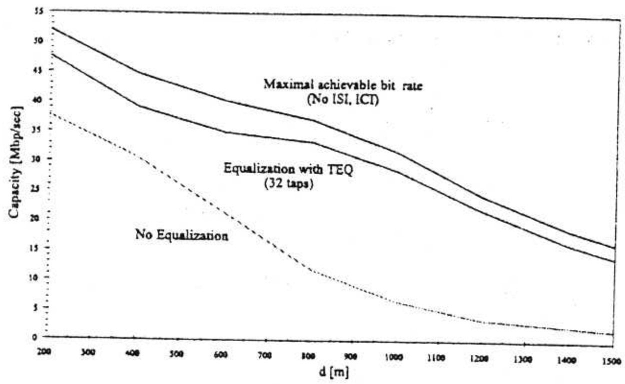

Fig. 7. Achievable bit rate as function of distance

The transmitter and receiver filters are 5-th order elliptic filters with 0.1 dB passband ripple and -69 dB stopband ripple. Fig. 4 depicts the composite impulse response of a 1 Km 24 AWG wire from which the tail and the head have been determined with the simplified synchronization algorithm (using the brick-wall window function). The magnitude of the FFT of the sampled head and tail is depicted in Fig. 5. Obviously, the largest ICI and ISI will appear on the carriers close to the cut-off frequency of the filters because of the large amplitude distortion and phase distortion about that frequency (located close to carrier 10). Fig. 6 depicts the received signal and noise spectra. In addition, the ICI_1, ICI_2 and ISI power on each carrier is depicted. Because of the long tail, the system performance is severely degraded by the ISI and ICI disturbance. On the average the ISI power is much smaller than the ICI except for carriers modulated near the cut-off frequency. The ICI, ISI interference level can be lowered by increasing the length of the prefix. This results into a smaller tail.

The guard band yields a reduction of the net data rate by a factor $\frac{\nu}{\nu+2N}$ which is negligible only when the DMT symbol period is taken sufficiently large. In practical systems however, the symbol duration is limited due to the maximal end-to-end transmission delay which is imposed by the application. In addition, larger symbol periods require more buffer capacity and a larger arithmetic complexity at the receiver. Alternatively, channel equalization can eliminate ISI and ICI. In [5] the performance of linear equalization is studied. Digital FIR filtering is applied to the received samples in order to shorten the composite channel impulse response to a fraction of the symbol period. The taps of the time domain equalizer (TEQ) are selected so that the impulse energy of the cascade of the channel and TEQ is concentrated in a time window smaller than the guard interval. Hence, the energy of the tail and head is reduced to a large extent. All presented expressions for ISI and ICI remain valid provided that the impulse response of the TEQ is taken into account. Fig. 7 depicts the achievable capacity as function of the length d of the copper wire according to (11) with a margin (M) of 6 dB and 3.5 dB coding gain (G). The upper curve depicts the maximal achievable bit rate in the assumption that a genius device at the receiver can eliminate all ICI and ISI. In the absence of a TEQ, a large capacity loss caused by ICI and ISI is observed whereas a 32 tap TEQ yields acceptable degradation.

V. Conclusions

In this paper, an analysis of the ISI and the ICI which is added to the decision variables when the length of the composite impulse response exceeds the prefix length is presented. It is shown that for multi-carrier transmission by means of modulated IDFT basis vectors, the interference can be expressed as function of the FFT on the head and tail of the composite impulse response. A simple symbol frame synchronization structure is derived based on minimizing the total ISI and ICI power. The results are applied to high rate data transmission over copper wires where the capacity loss caused by the presence of ISI and ICI is illustrated.

Acknowledgments

The first author expresses his gratitude to Alcatel Bell, B-2018, Antwerp, Belgium. The second author gratefully acknowledges the financial support from the Belgian National Fund for Scientific

Research (NFWO). The authors are indebted to Stijn Braet, Alcatel Telecom, for producing the simulation results.

APPENDIX

The ISI power summed over all carriers in the DMT signal, in the assumption that the $2N$ carriers are modulated can be expressed as

$$V_{\mathrm{ISI}}(\Delta) = \sum_{k'=0}^{2N-1} \mathrm{E}[|\mathrm{ISI}(m',k')|^2]$$

$$= \frac{E_s}{(2N)^2}\left[\sum_{k'=0}^{2N-1} |\mathrm{FFT}_1(k')+\mathrm{FFT}_3(k')|^2 + \sum_{k'=0}^{2N-1} |2N\mathrm{FFT}_2(k') - \mathrm{FFT}_4(k')|^2\right] \quad (A.1)$$

The first sum in (A.1) can be rewritten as

$$\frac{E_s}{(2N)^2}\sum_{k'=0}^{2N-1}\left|\sum_{n=\nu+1}^{2N+\nu}(n-\nu)g((n+\Delta)T)e^{-j\frac{2\pi}{2N}k'n}\right|^2$$

$$= \frac{E_s}{(2N)^2}\sum_{n=\nu+1}^{2N+\nu}\sum_{n'=\nu+1}^{2N+\nu}\sum_{k'=0}^{2N-1}(n-\nu)(n'-\nu)\cdot$$

$$g((n+\Delta)T)g((n'+\Delta)T)e^{-j\frac{2\pi}{2N}k'(n-n')}$$

$$= \frac{E_s}{2N}\sum_{k'=0}^{2N-1}\sum_{n=\nu+1}^{2N+\nu}(n-\nu)^2 g^2((n+\Delta)T) \quad (A.2)$$

Similarly, the second sum can be expressed as

$$\frac{E_s}{(2N)^2}\sum_{k'=0}^{2N-1}\left|\sum_{n=-2N}^{-1} ng((n+\Delta)T)e^{-j\frac{2\pi}{2N}k'n}\right|^2$$

$$= \frac{E_s}{2N}\sum_{n=-2N}^{-1} n^2 g^2((n+\Delta)T) \quad (A.3)$$

Combining (A.2) and (A.3) yields

$$V_{\mathrm{ISI}}(\Delta) = 2NE_s\sum_{n=-\infty}^{+\infty} w_{\mathrm{ISI}}(n)g^2((n+\Delta)T)$$

with the weight function $w_{\mathrm{ISI}}(n)$ as depicted in Fig 2. An equivalent approach can be applied for calculating the total ICI_1, ICI_2 power and total useful power V_{U}.

REFERENCES

[1] Weinstein S.B., Ebert P.M. *"Data transmission by frequency-division multiplexing using the discrete Fourier transform."* IEEE Trans. Commun., Oct. 1971, pp. 628-634.

[2] Pollet T., Moeneclaey M.. *"Synchronizability of OFDM Signals."* Globecom'95, Singapore, Vol. III, 13-17 Nov. 1995, pp. 2054-2058.

[3] Pollet T., Moeneclaey M., *"The effect of Carrier Frequency Offset on the Performance of Band limited Single Carrier and OFDM signals,"* Globecom'96, London, 18-22 Nov. 1996.

[4] Sandell M.,van de Beek JJ.. Borjesson P.O., *"Low-complex frame synchronization in OFDM systems,"* ICUPC'95, Nov. 1995.

[5] Al-Dhahir N.. Cioffi J. M., *"Efficiently Computed Reduced-Parameter Input-Aided MMSE Equalizers for ML Detection: A Unified Approach,"* IEEE Trans. on Inf. Theory, Vol. 42, No.3, pp 903-915, 1996.

[6] Pollet T., Spruyt P., Moeneclaey M., *"The BER Performance of OFDM Systems using Non-Synchronized Sampling,"* Globecom'94, San Francisco, pp. 253-257, 1994.

[7] Al-Dhahir N., Cioffi J. M.. *"Optimum Finite-length Equalization for Multicarrier Transceivers,"* IEEE Trans. on Commun., Vol. 44, No.1, pp 56-64,January 1996.

[8] Kalet I., *"The multitone channel,"* IEEE Trans. Commun., Vol. 37, No. 2, Feb. 1989, pp. 119-124.